On the use of slope limiters for the design of recovery based error indicators

M. Möller[1] and D. Kuzmin[2]

[1] Institute of Applied Mathematics (LS III), University of Dortmund, Vogelpothsweg 87, D-44227 Dortmund, Germany
matthias.moeller@math.uni-dortmund.de
[2] kuzmin@math.uni-dortmund.de

Summary. A slope limiting approach to the design of recovery based *a posteriori* error indicators for P_1 finite element discretizations is presented. The smoothed gradient field is recovered at edge midpoints by means of limited averaging of adjacent slope values. As an alternative, the constant gradient values may act as upper and lower bounds to be imposed on edge gradients resulting from traditional reconstruction techniques such as averaging projection or discrete patch recovery schemes. In either case, the difference between consistent and reconstructed gradient values measured in the L_2-norm provides a usable indicator for grid adaptivity.

1 Introduction

In a series of recent publications (c.f. [3], [4] and the references therein) an algebraic framework for the construction of high-resolution schemes for convection dominated partial differential equations was developed. The *algebraic flux correction* (AFC) paradigm renders a high-order discretization local extremum diminishing (LED) by applying discrete (anti-)diffusion in a nonlinear conservative fashion. The antidiffusive fluxes are limited node-by-node either by a symmetric FCT limiter or by its upwind-biased counterpart of TVD type.

The adaptive blending of high- and low-order methods prevents us from using error estimators that require an *a priori* knowledge of the order of approximation such as those based on Richardson extrapolation. Gradient recovery techniques [8] seem to be a promising alternative, but their use in error estimation requires that the true solutions be sufficiently smooth.

This paper focuses on hyperbolic problems featuring shocks and discontinuities so that traditional recovery procedures may fail to be reliable. In what follows, limited averaging of consistent slopes is used to compute improved gradient values at midpoints of edges. As an alternative, classical recovery procedures are employed to predict provisional gradient values at edge midpoints to be corrected by means of a slope limiter. The upper and lower bounds to be imposed are given by the constant slopes in two adjacent triangles.

2 A posteriori error indication

As a model problem, consider the weak form of a generic PDE $\mathcal{L}\mathrm{u} = f$

$$\int_\Omega w[\mathcal{L}\mathrm{u} - f]\,\mathrm{d}\mathbf{x} = 0 \tag{1}$$

where the solution is approximated by means of finite elements

$$\mathrm{u} \approx u_h = \sum_j u_j \varphi_j. \tag{2}$$

In this article, we shall concentrate on the numerical error resulting from the *approximation* of spatial derivatives and devise an *a posteriori* indicator for the vector-valued gradient error $\mathbf{e} = \nabla\mathrm{u} - \nabla u_h$. In the sequel, the consistent gradient $\nabla u_h = \sum_j u_j \nabla\varphi_j$ will be referred to as low-order gradient.

The aim of recovery based error estimators, introduced by Zienkiewicz and Zhu in [8], is to replace the unknown exact value $\nabla\mathrm{u}$ by a smoothed gradient field $\hat{\nabla} u_h$, so as to obtain a good approximation to the true error

$$\mathbf{e} \approx \hat{\mathbf{e}} = \hat{\nabla} u_h - \nabla u_h. \tag{3}$$

In general, pointwise error estimates are difficult to obtain, so integral measures are typically employed in the finite element framework. Let Ω_h denote a partition of the domain into a set of non-overlapping elements Ω_e so that the L_2-norm represents a usable measure for the error both globally and locally

$$||\hat{\mathbf{e}}||_{L_2}^2 = \sum_{\Omega_e} ||\hat{\mathbf{e}}||_{L_2(\Omega_e)}^2, \qquad ||\hat{\mathbf{e}}||_{L_2(\Omega_e)}^2 = \int_{\Omega_e} \hat{\mathbf{e}}^{\mathrm{T}}\hat{\mathbf{e}}\,\mathrm{d}\mathbf{x}. \tag{4}$$

We only consider linear (P_1) finite elements for which the consistent gradient ∇u_h is piecewise constant on each triangle. Hence, the improved slopes should be at least piecewise linear so as to provide a better approximation to the exact gradient. It suffices to specify slope values at all midpoints of edges, i.e., $\mathbf{x}_{ij} := \frac{1}{2}(\mathbf{x}_i + \mathbf{x}_j)$, to obtain a smoothed quantity $\hat{\nabla} u_h$ that varies linearly in Ω_e and is allowed to exhibit jumps across interelement boundaries. This approach can be seen as determining the nodal values for a non-conforming approximation of $\hat{\nabla} u_h$ by means of linear Crouzeix-Raviart finite elements for which the local degrees of freedom are located on edge midpoints. For bilinear finite elements used on quadrilateral meshes, the gradient approximation can be based on the nonconforming Rannacher Turek element.

Let (4) be integrated via the second order accurate quadrature rule

$$\int_{\Omega_e} \hat{\mathbf{e}}^{\mathrm{T}}\hat{\mathbf{e}}\,\mathrm{d}\mathbf{x} = \frac{|\Omega_e|}{3}\sum_{ij} \hat{\mathbf{e}}_{ij}^{\mathrm{T}}\hat{\mathbf{e}}_{ij}, \qquad \hat{\mathbf{e}}_{ij} = \hat{\nabla} u_{ij} - \nabla u_{ij}, \tag{5}$$

where $|\Omega_e|$ stands for the element area and all quantities are evaluated at the midpoints of surrounding edges indicated by subscript ij. It remains to devise a procedure for constructing an improved gradient value $\hat{\nabla} u_{ij}$ for edge **ij**.

3 Limited gradient averaging

Our first approach to obtaining a smoothed edge gradient is largely inspired by slope limiting techniques employed in the context of high-resolution finite volume schemes and later carried over to discontinuous Galerkin finite element methods. For simplicity, let us illustrate the basic ideas for a one-dimensional finite volume discretization. The task is to define a suitable slope value u'_j on the jth interval $I_j = (x_{j-1/2}, x_{j+1/2})$ so as to recover a piecewise linear approximate solution from the mean value $\bar{u}_j$:

$$u_h(x) = \bar{u}_j + u'_j(x - x_j), \qquad \forall\, x \in I_j. \tag{6}$$

In the simplest case, one-sided or centered slopes can be utilized to obtain first- and second-order accurate schemes which lead to rather diffusive profiles and are quite likely to produce nonphysical oscillations in the vicinity of steep fronts and discontinuities, respectively. For a numerical scheme to be nonoscillatory, it should possess certain properties [3], e.g., be monotone, positivity preserving, total variation diminishing or satisfy the LED condition.

To this end, Jameson [2] introduced a family of limited average operators $\mathcal{L}(a, b)$ which are characterized by the following properties:

P1. $\mathcal{L}(a, b) = \mathcal{L}(b, a)$.
P2. $\mathcal{L}(ca, cb) = c\mathcal{L}(a, b)$.
P3. $\mathcal{L}(a, a) = a$.
P4. $\mathcal{L}(a, b) = 0$ if $ab \leq 0$.

While conditions P1–P3 are natural properties of an average, P4 is to be enforced by means of a limiter function. It has been demonstrated [2] that a variety of standard TVD limiters can be written in such form. Let the modified sign function be given by $\mathcal{S}(a, b) = \frac{1}{2}(\mathrm{sign}(a) + \mathrm{sign}(b))$ which equals zero for $ab \leq 0$ and returns the common sign of a and b otherwise. Then the most widely used two parameter limiters for TVD schemes can be written as:

1. minmod:	$\mathcal{L}(a, b) = \mathcal{S}(a, b)\ \min\{\lvert a\rvert, \lvert b\rvert\}$
2. maxmod:	$\mathcal{L}(a, b) = \mathcal{S}(a, b)\ \max\{\lvert a\rvert, \lvert b\rvert\}$
3. MC:	$\mathcal{L}(a, b) = \mathcal{S}(a, b)\ \min\left\{\frac{1}{2}\lvert a + b\rvert, 2\lvert a\rvert, 2\lvert b\rvert\right\}$
4. superbee:	$\mathcal{L}(a, b) = \mathcal{S}(a, b)\ \max\{\min\{2\lvert a\rvert, \lvert b\rvert\}, \min\{\lvert a\rvert, 2\lvert b\rvert\}\}$

Finally, the limited counterpart of u'_j in (6) can be computed as follows

$$\hat{u}'_j = \mathcal{L}\left(\frac{\bar{u}_{j-1} - \bar{u}_j}{x_{j-1} - x_j}, \frac{\bar{u}_{j+1} - \bar{u}_j}{x_{j+1} - x_j}\right). \tag{7}$$

Let us return to our original task that requires the reconstruction of solution gradients at edge midpoints. This is where the benefits of an edge based formulation come into play. Except at the boundary, *exactly* two elements

are adjacent to edge **ij** such that an improved gradient can be determined efficiently from the constant slopes to the left and to the right as follows:

$$\hat{\nabla} u_{ij} = \mathcal{L}(\nabla u_{ij}^{+}, \nabla u_{ij}^{-}). \tag{8}$$

For all limiter functions $\mathcal{L}$ presented above, the recovered gradient value equals zero if $\nabla u_{ij}^{+} \nabla u_{ij}^{-} \leq 0$ and satisfies the following inequality otherwise

$$\nabla u_{ij}^{\min} \leq \hat{\nabla} u_{ij} \leq \nabla u_{ij}^{\max}, \qquad \text{where} \qquad \nabla u_{ij}^{\substack{\max \\ \min}} = \begin{matrix} \max \\ \min \end{matrix} \{\nabla u_{ij}^{+}, \nabla u_{ij}^{-}\}. \tag{9}$$

If the upper and lower bounds have different signs, this indicates that the approximate solution attains a local extremum across the edge. Hence, property P4 of limited average operators acts as a discrete analog to the necessary condition in the continuous case which requires the derivative to be zero.

Clearly, the recovered gradient (8) depends on the choice of the limiter function to some extent. In the authors' experience, MC seems to be a safe choice as it tries to select the standard average whenever possible without violating the natural bounds provided by the low-order slopes.

4 Limited gradient reconstruction

As an alternative to the limited averaging approach, traditional recovery procedures can be used to *predict* provisional gradient values at edge midpoints which are *corrected* by edgewise slope limiting so as to satisfy the geometric constraints defined in (9). Since the advent of recovery based schemes [8], a family of *averaging projection* schemes has been proposed in the literature to construct a smoothed gradient from the finite element solution as follows

$$\hat{\nabla} u_h = \sum_j \hat{\nabla} u_j \phi_j, \tag{10}$$

where the coefficients $\hat{\nabla} u_j$ are obtained by solving the discrete problem

$$\int_\Omega \phi_i (\hat{\nabla} u_h - \nabla u_h) \, \mathrm{d}\mathbf{x} = 0. \tag{11}$$

Note that the element shape functions used to construct the basis functions ϕ_i may by different from those used in the finite element approximation (2). A detailed analysis by Ainsworth *et. al.* [1] reveals that the corresponding polynomial degrees should satisfy $\deg \phi \geq \deg \varphi$ whereby the original choice $\phi = \varphi$ proposed in [8] 'is not only effective, but also the most economical' [1] one. The substitution of equation (10) into (11) yields a linear algebraic system for each component of the smoothed gradient

$$M_C \hat{\nabla} u_h = \mathbf{C}\, u. \tag{12}$$

The consistent mass matrix $M_C = \{m_{ij}\}$ and the matrix of discretized spatial derivatives $\mathbf{C} = \{\mathbf{c}_{ij}\}$ are assembled from the following integral terms

$$m_{ij} = \int_\Omega \phi_i \varphi_j \,\mathrm{d}\mathbf{x}, \qquad \mathbf{c}_{ij} = \int_\Omega \phi_i \nabla\varphi_j \,\mathrm{d}\mathbf{x}. \tag{13}$$

For a fixed mesh, the coefficients m_{ij} and $\mathbf{c}_{ij}$ remain unchanged throughout the simulation and, consequently, need to be evaluated just once at the beginning of the simulation and each time the grid has been modified. In case $\phi \equiv \varphi$, the coefficients defined in (13) coincide with the matrix entries of the finite element approximation and, hence, are available at no additional costs.

An edge-by-edge assembly of the right-hand side is also feasible

$$(\mathbf{C}\,u)_i = \sum_{j\neq i} \mathbf{c}_{ij}(u_j - u_i) \tag{14}$$

since $\mathbf{C}$ features the zero row sum property $\sum_j \mathbf{c}_{ij} = 0$ as long as the sum of basis functions equals one. The solution to system (12) can be computed iteratively by successive approximation preconditioned by the lumped mass matrix $M_L = \mathrm{diag}\{m_i\}$, where $m_i = \sum_j m_{ij}$, as follows:

$$\hat{\nabla} u_h^{(m+1)} = \hat{\nabla} u_h^{(m)} + M_L^{-1}[\mathbf{C}\,u - M_C \hat{\nabla} u_h^{(m)}], \qquad m = 0, 1, 2, \ldots. \tag{15}$$

If mass lumping is applied directly to equation (12), the values of the projected gradient can be determined at each node from the explicit formula

$$\hat{\nabla} u_i = \frac{1}{m_i} \sum_{j\neq i} \mathbf{c}_{ij}(u_j - u_i). \tag{16}$$

From the nodal values obtained either from (12) or (16), provisional slopes at edge midpoints can be interpolated according to equation (10). For linear finite elements this corresponds to taking the mean values for each edge **ij**, i.e., $\hat{\nabla} u_h(\mathbf{x}_{ij}) := \frac{1}{2}(\hat{\nabla} u_i + \hat{\nabla} u_j)$. It follows from (10) and (11) that it is also feasible to project the low-order gradient ∇u_h into the space of non-conforming (bi-) linear finite element by letting $\phi_j \in \tilde{P}_1$ or $\tilde{Q}_1$, respectively, so as to obtain its smoothed counterpart directly at edge midpoints.

Over the years, a more accurate patch recovery technique (SPR) was introduced [9] which relies on the superconvergence property of the finite element solution at some exceptional, yet *a priori* known, points. Let the smoothed gradient be represented in terms of a polynomial expansion of the form

$$\hat{\nabla} u_h = p(\mathbf{x})\mathbf{a} \tag{17}$$

where the row vector $p(\mathbf{x})$ contains all monomials of degree k at most. Since each vertex, say i, is surrounded by a patch of elements sharing this node, the vector of coefficients $\mathbf{a}$ can be computed from a discrete least square fit to

the set $\mathcal{S}_i$ of sampling points $\mathbf{x}_j$ [9]. As a consequence, the multicomponent quantity $\mathbf{a}$ can be determined by solving the linear system

$$M_p\,\mathbf{a} = \mathbf{f}, \tag{18}$$

where the local matrix M_p and the right-hand side vector $\mathbf{f}$ are given by

$$M_p = \sum_{j\in\mathcal{S}_i} p^{\mathrm{T}}(\mathbf{x}_j)\,p(\mathbf{x}_j), \qquad \mathbf{f} = \sum_{j\in\mathcal{S}_i} p^{\mathrm{T}}(\mathbf{x}_j)\,\nabla u_h(\mathbf{x}_j). \tag{19}$$

For linear elements, $p(\mathbf{x}) = [1, x, y]$ and the low-order gradient is sampled at the centroids of triangle in the patch. In this case the lumped L_2-projection yields almost the same results on uniform grids but only patch recovery retains its superconvergence property if the grid becomes increasingly distorted.

Regardless of which procedure is employed to predict the high-order gradient values, it may fail if the solution exhibits jumps or the gradient is too steep. This can be attributed to the fact that the averaging process extends over an *unsettled* number of surrounding element gradients which may strongly vary in magnitude and even possess different signs. Thus, it is very difficult the find admissible bounds to be imposed on such *nodal* gradients. The transition to an edge based formulation makes it possible to correct the provisional values according to the constraints (9), set up by the low-order slopes, such that

$$\nabla u_{ij}^{\min} \le \hat{\nabla} u_{ij} \le \nabla u_{ij}^{\max}. \tag{20}$$

It is also advisable to enforce the sign-preserving property (P4) of limited average operators so as to mimic the necessary condition of a local extremum attained across edge **ij** in the discrete context. Let $s_{ij} := \mathcal{S}(\nabla u_{ij}^{\min}, \nabla u_{ij}^{\max})$, then the corrected slope values $\hat{\nabla} u_{ij}^{*}$ can be computed as follows:

$$\hat{\nabla} u_{ij}^{*} = s_{ij}\left|\max\{\nabla u_{ij}^{\min}, \min\{\hat{\nabla} u_{ij}, \nabla u_{ij}^{\max}\}\}\right| \tag{21}$$

The generality of this predictor-corrector *edgewise limited recovery* (ELR) approach, enables us to use arbitrary reconstruction techniques in the prediction step, e.g., polynomial preserving recovery (PPR) [6] schemes or some recent 'meshless' variants which have been presented by Zhang *et. al.* [7].

5 Adaptation strategy

In adaptive solution procedures for steady state simulations of hyperbolic flows, one typically starts with a moderately coarse grid on which an initial solution can be computed efficiently. Nevertheless, the mesh needs to be fine enough in order to capture all essential flow features in the solution and to enable the error indicator to detect 'imperfect' zones. Next, the grid is locally

refined or coarsened according to some adaptation parameter and the whole process is repeated until (ideally) the global relative percentage error

$$\eta := \frac{||\mathbf{e}||_{L_2}}{||\nabla u||_{L_2}} \leq \eta_{\text{tol}} \tag{22}$$

is below the prescribed tolerance η_{tol}. Replacing the unknown exact quantities by their approximate values and assuming that the relative error is distributed equally between cells the gradient error for each element Ω_e should not exceed

$$||\hat{\mathbf{e}}||_{L_2(\Omega_e)} \leq \eta_{\text{tol}} \left[\frac{||\nabla u_h||^2_{L_2} + ||\hat{\mathbf{e}}||^2_{L_2}}{|\Omega_h|} \right]^{1/2}, \tag{23}$$

where $|\Omega_h|$ represents the number of employed elements. Depending on the ratio of estimated and tolerated error, cells are flagged for refinement or coarsening. For a detailed presentation of the grid adaptation procedure including some grid improvement techniques the interested reader is referred to [5].

6 Numerical examples

Let us illustrate the performance of the new algorithm by considering a supersonic flow which enters a converging channel at $M_\infty = 2$. The bottom wall is sloped at 5° which gives rise to the formation of multiple shock reflections. The initial mesh consist of 60×16 quadrilaterals each of which is divided into two triangles. After three sweeps of local mesh refinement ($\eta_{\text{ref}} = 1\%$) and coarsening ($\eta_{\text{crs}} = 0.1\%$) governed by the MC-limited averaging error indicator, the zone of highest grid point concentration confines itself more and more to the vicinity of the shock as depicted in Figure 1. Algebraic flux correction of TVD type [4] was employed to compute the solution, making use of the moderately diffusive CDS-limiter applied to the characteristic variables.

The density distribution for the finest grid (15,664 elements) demonstrates the precise separation into five zones of uniform flow. The crisp resolution of the reflected shock wave can also be observed by considering the density 'cascade' drawn along the straight line $y = 0.6$ for all four grid levels.

7 Conclusions

Slope limiting techniques provide a valuable tool for the construction of high-resolution gradient recovery procedures. Improved slopes can be directly computed at edge midpoints as a limited average of adjacent low-order gradients. Moreover, the consistent slope values serve as natural upper and lower bounds to be imposed on any edge gradient. In addition, traditional (nodal) recovery procedures can be used to predict the high-order gradient which is corrected according to geometric constraints by invoking a slope limiter edge-by-edge.

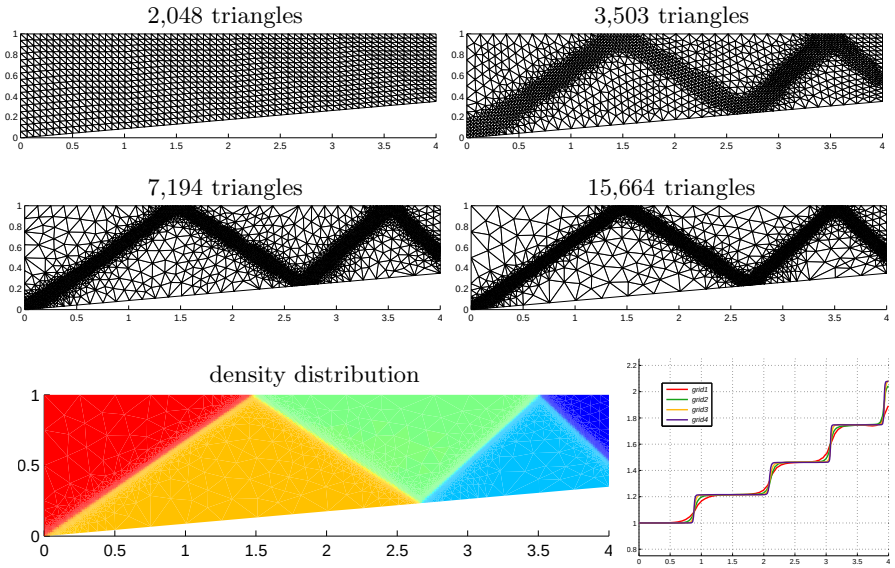

Fig. 1. 5° converging channel at $M_\infty = 2$

References

1. M. Ainsworth, J.Z. Zhu, A.W. Craig, O.C. Zienkiewicz, Analysis of the Zienkiewicz-Zhu a-posteriori error estimator in the finite element method. *Int. J. Numer. Meth. Engng.* **28** (1989) 2161–2174.
2. A. Jameson, Analysis and design of numerical schemes for gas dynamics 1. Artificial diffusion, upwind biasing, limiters and their effect on accuracy and multigrid convergence. *Int. Journal of CFD* **4** (1995) 171–218.
3. D. Kuzmin, M. Möller, Algebraic flux correction I. Scalar conservation laws. In: D. Kuzmin, R. Löhner, S. Turek (eds.) *Flux-Corrected Transport: Principles, Algorithms, and Applications*. Springer, 2005, 155–206.
4. D. Kuzmin, M. Möller, Algebraic flux correction II. Compressible Euler equations. In: D. Kuzmin, R. Löhner, S. Turek (eds.) *Flux-Corrected Transport: Principles, Algorithms, and Applications*. Springer, 2005, 207–250.
5. M. Möller, D. Kuzmin, Adaptive mesh refinement for high-resolution finite element schemes. Submitted to: *Int. J. Numer. Meth. Fluids*.
6. A. Naga, Z. Zhang, A Posteriori error estimates based on polynomial p reserving recovery. *SIAM J. Numer. Anal.* **42** (2004) 1780–1800.
7. Z. Zhang, A. Naga, A new finite element gradient recovery method: Sup ercon-vergence property. *SIAM J. Sci. Comput.* **26** (2005) 1192–1213.
8. O.C. Zienkiewicz, J.Z. Zhu, A simple error estimator and adaptive procedure for practical engineering analysis. *Int. J. Numer. Methods Eng.* **24** (1987) 337–357.
9. O.C. Zienkiewicz, J.Z. Zhu, The superconvergent patch recovery and a posteriori error estimates. Part 1: The recovery techniques. *Int. J. Numer. Methods Eng.* **33** (1992) 1331–1364.